Reduction of Bend Losses at Sharp Bend in Post Wall Waveguide

Ken'ichiro Yashiro[1] **and Ning Guan**[2]

[1]Chiba University, Japan
[2]Fujikura Ltd., Japan

Abstract— In this paper, we consider some techniques to reduce the bend losses. We apply the method of moments to analyse the reflection of millimeter waves from the right-angle bend. The global basis functions were used to reduce the number of unknowns per metal post and the necessary computer memory is also reduced. Furthermore, the Galerkin method was used to obtain a sytem of linear equations. Therefore, the resulting matrix is symmetric. Since the objects were confined to circular metallic posts, the elements of matrix were calculated in closed form and no numerical integration is needed.

It will be shown that only a few additional posts are set at appropriate positions in the post wall waveguide, almost all incident waves go around the corner and the bend losses are minimized. Especially, only one additional metallic post is enough to minimize the bend losses.

1. INTRODUCTION

A post wall waveguide is a promising candidate for the development of low cost circuits in the millimetre-wave region. Recently, the integrated-waveguide scheme was proposed by Hirokawa et al. and the feed waveguide for a parallel-plate slot array antenna was composed of densely arrayed posts on the same layer as the parallel plates [1]. The integrated-waveguide filter was demonstrated by using the post-wall waveguide technique [2].

The post-wall waveguide consists of two rows of metal posts sandwiched between two parallel metal plates as shown in Figure 1. In some instances, the post-wall waveguide may be bent to fabricate millimeter-wave integrated circuits. Various bend geometries was introduced [3]. These geometries include the right-angle bend with a via, chamfered bend and rounded bend. The influence of the geometry of the chamfered bends was investigated by HFSS and the transmission coefficients S_{21} were determined [4].

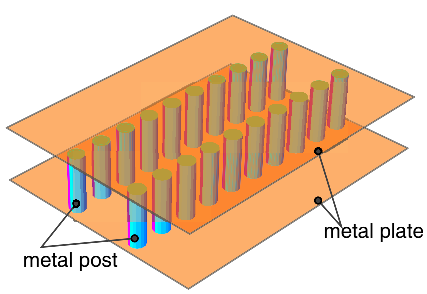

Figure 1: Post-wall waveguide.

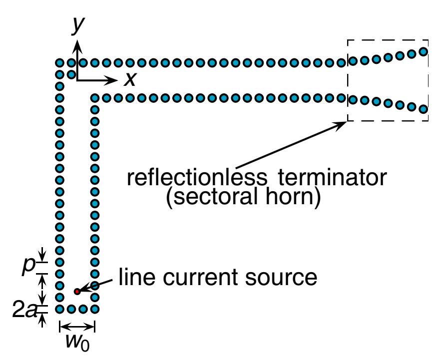

Figure 2: Geometry of problem.

In this paper, we consider some geometries of bends to reduce the bend losses. We will analyse the reflections from the right-angle bend. The method of moments (MoM) with global base [5] is used to obatin the distribution of electromagnetic fields. The global basis functions were used to reduce the number of unknowns per metal post and the necessary computer memory is also reduced. Furthermore, the Galerkin method was used to obtain a sytem of linear equations. Therefore, the resulting matrix is symmetric. Since the objects were confined to circular metallic posts, the elements of matrix were calculated in closed form and no numerical integration is needed. The standing waves will be computed and the reflections from the bends are evaluated from the voltage standing wave ratio (VSWR).

2. FORMULATION

The geometry of the problem consists of N posts as illustrated in Figure 2. Suppose that the incident plane wave is a cylindrical wave radiated from a line current source located at (x_0, y_0). One end of the waveguide is short-terminated behind the line source and the other end is connected to a H-plane sectoral horn, which works as reflectionless terminator.

The electromagnetic fields are assumed to be uniform along z-axis. A time dependence $e^{j\omega t}$ is assumed and suppressed throughout. Then the incident wave is assumed to be expressed as

$$E_z^i(\vec{\rho}) = \frac{E_0}{j4} H_0^{(2)}(k_0|\vec{\rho} - \vec{\rho}_0|) \tag{1}$$

where $H_0^{(2)}(x)$, k_0 and $\vec{\rho}_0$ are the Hankel function of the second kind of 0-th order, the wave number and a location of source, respectively. Let $J_z^\nu(\vec{\rho})$ be the current density on the ν-th cylinder of which cross-section has a circumference C_ν with a radius a_ν. Then the scattered wave is described by

$$E_z^s(\vec{\rho}) = -\frac{k_0\zeta_0}{4} \cdot \sum_{\nu=1}^{N} \int_{C_\nu} H_0^{(2)}(k_0|\vec{\rho} - \vec{\rho}\,'|) J_z^\nu(\vec{\rho}\,') d\rho' \tag{2}$$

where $\zeta_0(= \sqrt{\mu_0/\varepsilon_0})$ is the intrinsic impedance of free space. The total tangential component of electric fields vanishes on every post surface. Hence,

$$E_z^s(\vec{\rho}) = -E_z^i(\vec{\rho}), \quad \vec{\rho} \in C_\nu \ (\nu = 1, 2, \ldots, N) \tag{3}$$

Equation (3) give a system of boundary integral equations.

Here we introduce a local polar coordinate system $(r_\nu,\ \theta_\nu)$ of which origin is the center of C_ν, i.e., $\vec{\rho}_\nu$. Then $\vec{\rho} = \vec{\rho}_\nu + \vec{r}_\nu$. Since the current density should be periodic along C_ν, each current is expanded in terms of a set of global basis functions $e^{-jn\theta_\nu}$ as

$$J_z^\nu(\vec{\rho}\,') = E_0 \sum_{n=-N_\nu}^{N_\nu} \chi_n^\nu e^{-jn\theta_\nu'} \tag{4}$$

Substituting (4) into (2) and using Graf's addition theorem [6]

$$H_n^{(2)}(k_0R) \begin{matrix}\cos\\ \sin\end{matrix} n\psi = \sum_{m=-\infty}^{\infty} H_{n+m}^{(2)}(k_0R_\nu) J_m(k_0a_\nu) \begin{matrix}\cos\\ \sin\end{matrix} m\varphi \tag{5}$$

we integrate the resulting equation to obtain

$$E_z^s(\vec{\rho}) = -E_0 \frac{\pi k_0\zeta_0}{2} \sum_{\nu=1}^{N} \sum_{n=-N_\nu}^{N_\nu} \chi_n^\nu a_\nu J_n(k_0a_\nu) H_n^{(2)}(k_0R_\nu) e^{-jn\theta_\nu} \tag{6}$$

where $R_\nu = |\vec{\rho} - \vec{\rho}_\nu|$, θ_ν is an angle between $\vec{\rho} - \vec{\rho}_\nu$ and x-axis. Three points $\vec{\rho}$, $\vec{\rho}\,'$, $\vec{\rho}_\nu$ form a triangle with sides, $\vec{\rho} - \vec{\rho}\,'$, $\vec{\rho} - \vec{\rho}_\nu$, $\vec{\rho}\,' - \vec{\rho}_\nu$, and ψ and φ are vertex angles opposite to $\vec{\rho}\,' - \vec{\rho}_\nu$ and $\vec{\rho} - \vec{\rho}\,'$, respectively.

We take an inner product of (3) with a set of weighting functions to obtain a matrix equation. The basis functions are also chosen as weighting functions. In other words, the Galerkin's method is used. By using Graf's addition theorem, the right side of the inner product of (3) with $e^{jm\theta_\mu}$ yields

$$-\int_{C_\mu} E_z^i(\vec{\rho}) e^{jm\theta_\mu} d\rho = -\frac{\pi}{j2k_0} E_0 (-1)^m k_0 a_\mu J_m(k_0a_\mu) H_m^{(2)}(k_0R_{\mu 0}) e^{jm\alpha_{\mu 0}} \tag{7}$$

where $R_{\mu 0} = |\vec{\rho}_\mu - \vec{\rho}_0|$, and $\alpha_{\mu 0}$ is an angle between $\vec{\rho}_\mu - \vec{\rho}_0$ and x-axis.

The left side of the inner product of (3) with $e^{jm\theta_\mu}$ does not depend on the incident wave except χ_n^ν. Hence its integration is carried out in the same way as the case of incident plane wave in [5].And the resulting matrix equation is given by

$$\begin{bmatrix} A_{11} & A_{12} & \ldots & A_{1N} \\ A_{21} & A_{22} & \ldots & A_{2N} \\ \cdot & \cdot & \ldots & \cdot \\ A_{N1} & A_{N2} & \ldots & A_{NN} \end{bmatrix} \begin{bmatrix} X_1 \\ X_2 \\ \cdot \\ X_N \end{bmatrix} = \begin{bmatrix} B_1 \\ B_2 \\ \cdot \\ B_N \end{bmatrix} \tag{8}$$

where $A_{\nu\nu}$ and $A_{\mu\nu}$ are $(2N_\nu+1)\times(2N_\nu+1)$ diagonal matrix and $(2N_\mu+1)\times(2N_\nu+1)$ matrix, respectively, and X_ν and B_ν are $2N_\nu+1$ column vectors, and their elements are given as follows:

$$a_{mn}^{\nu\nu} = -\frac{\pi^2\zeta_0}{k_0}(k_0a_\nu)^2 J_n(k_0a_\nu)H_n^{(2)}(k_0a_\nu)\delta_{mn} \tag{9}$$

$$a_{mn}^{\mu\nu} = -\frac{\pi^2\zeta_0}{k_0}k_0a_\mu k_0a_\nu J_m(k_0a_\mu)J_n(k_0a_\nu)H_{n-m}^{(2)}(k_0R_{\mu\nu})e^{-j(n-m)\alpha_{\mu\nu}} \tag{10}$$

$$b_m^\mu = -\frac{\pi}{j2k_0}(-1)^m k_0a_\mu J_m\left(k_0a_\mu\right)H_m^{(2)}\left(k_0R_{\mu 0}\right)e^{jm\alpha_{\mu 0}} \tag{11}$$

where δ_{mn} is the Kronecker delta, $R_{\mu\nu}=|\vec{\rho}_\mu-\vec{\rho}_\nu|$, and $\alpha_{\mu\nu}$ is an angle between $\vec{\rho}_\mu-\vec{\rho}_\nu$ and x-axis.

The magnetic fields can be calculated from the Maxwell equation.

$$H_x^i(\vec{\rho}) = -\frac{E_0}{4\zeta_0}H_1^{(2)}(k_0|\vec{\rho}-\vec{\rho}_0|)\frac{y-y_0}{|\vec{\rho}-\vec{\rho}_0|} = -\frac{E_0}{4\zeta_0}H_1^{(2)}(k_0|\vec{\rho}-\vec{\rho}_0|)\sin\theta_0 \tag{12}$$

$$H_y^i(\vec{\rho}) = \frac{E_0}{4\zeta_0}H_1^{(2)}(k_0|\vec{\rho}-\vec{\rho}_0|)\frac{x-x_0}{|\vec{\rho}-\vec{\rho}_0|} = \frac{E_0}{4\zeta_0}H_1^{(2)}(k_0|\vec{\rho}-\vec{\rho}_0|)\cos\theta_0 \tag{13}$$

$$\begin{aligned} H_x^s(\vec{\rho}) = -E_0\frac{\pi}{2}\sum_{\nu=1}^{N}\Bigg\{&\cos\theta_\nu\sum_{n=-N_\nu}^{N_\nu}\chi_n^\nu k_0a_\nu J_n(k_0a_\nu)e^{-jn\theta_\nu}\frac{n}{k_0R_\nu}H_n^{(2)}(k_0R_\nu) \\ &+j\sin\theta_\nu\sum_{n=-N_\nu}^{N_\nu}\chi_n^\nu k_0a_\nu J_n(k_0a_\nu)e^{-jn\theta_\nu}H_n^{(2)\prime}(k_0R_\nu)\Bigg\} \end{aligned} \tag{14}$$

$$\begin{aligned} H_y^s(\vec{\rho}) = -E_0\frac{\pi}{2}\sum_{\nu=1}^{N}\Bigg\{&-j\cos\theta_\nu\sum_{n=-N_\nu}^{N_\nu}\chi_n^\nu k_0a_\nu J_n(k_0a_\nu)e^{-jn\theta_\nu}H_n^{(2)\prime}(k_0R_\nu) \\ &+\sin\theta_\nu\sum_{n=-N_\nu}^{N_\nu}\chi_n^\nu k_0a_\nu J_n(k_0a_\nu)e^{-jn\theta_\nu}\frac{n}{k_0R_\nu}H_n^{(2)}(k_0R_\nu)\Bigg\} \end{aligned} \tag{15}$$

3. NUMERICAL RESULTS

For numerical computation, all the lengths are normalized by the wavelength in free space. The following values are used: $a=0.05\lambda$, $p=0.2\lambda$ and $w_0=0.6\lambda$, where λ is the wavelength in free space.

If the reflection at the open end of the post wall waveguide is large, it is difficult to evaluate qualitatively the reflected wave from the bend. Therefore, an H-plane sectoral horn is connected to the open end of the waveguide in order to reduce the reflected waves there. It is known [7] that a family of hyperbolic horns have the cross-sectional area S related to the distance x through the hyperbolic functions. Hence, the width w of horn can be given by

$$w = w_0\left(\cosh\alpha x + T\sinh\alpha x\right) \tag{16}$$

where w_0 is the width of waveguide, and α and T are constants. For $T=1$, the horn is an exponential horn.

The electric field distributions in the straight waveguide excited by a line current source are shown in Figure 3. Figure 3(a) shows the amplitude distribution of electric field in the post wall waveguide terminated with open end. It is seen from Figure 3(a) that some part of the enegy is reflected at the open end and standing waves are created. A horn is connected to the open end of waveguide so that the change in impedance at the end of a waveguide is gradual. Figure 3(b) shows the amplitude distribution of electric field in the post wall waveguide terminated with horn. We can see from the figure that almost no standing waves are formed.

Here, the horn is adopted as a reflectionless terminator. So the type of horn used is chosen according to the voltage standing wave ratio (VSWR). The length of horn is set to be 6λ long. Figure 4 shows the VSWR as a function of the parameter α with $T=0.2$. The VSWR for the waveguide terminated with open end is also shown in Figure 4. For the waveguide terminated with open end, the VSWR is 2.193 and the reflection coefficient $|\Gamma|=(VSWR-1)/(VSWR+1)$ is 0.374. However, the reflections at the end of waveguide is suppressed by terminating the horn.

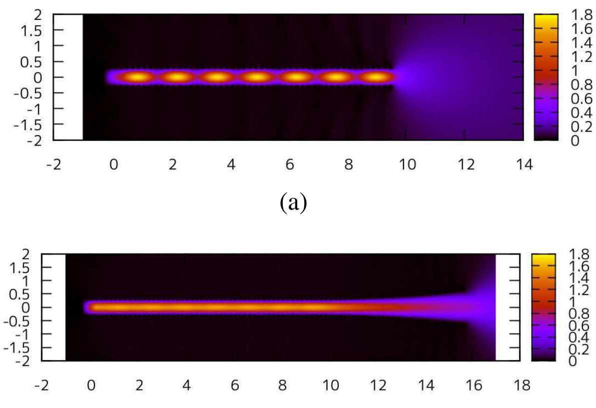

(a) (b)

Figure 3: Electric field distribution in terminated post wall waveguide. (a) Waveguide terminated with open end. (b) Waveguide terminated with horn.

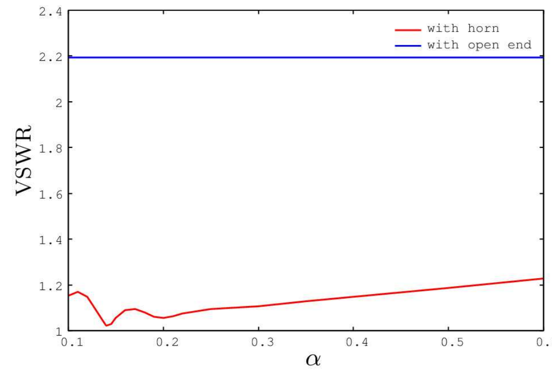

Figure 4: VSWR for post wall waveguide terminated by hyperbolic horn.

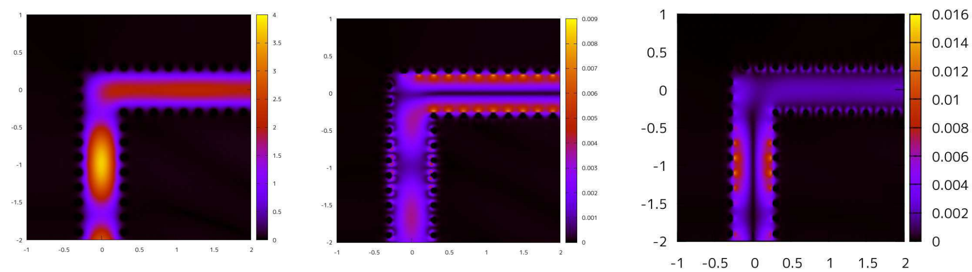

(a) $|E_z|$ (b) $|H_x|$ (c) $|H_y|$

Figure 5: Amplitude distributions of electromagnetic fields near right-angle bend.

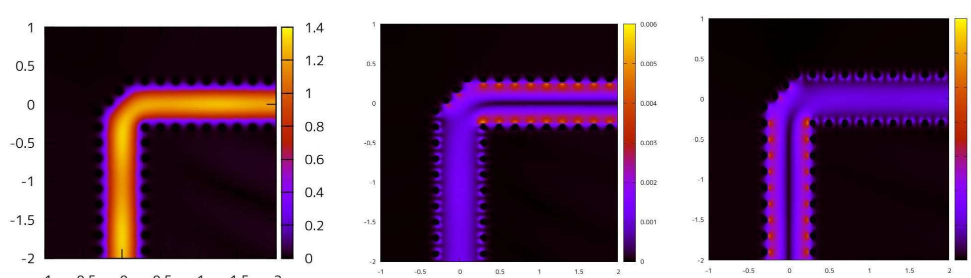

(a) $|E_Z|$ (b) $|H_X|$ (c) $|H_Y|$

Figure 6: Amplitude distributions of electromagnetic fields near the type A of the bend.

The VSWR is 1.055 for horn with $\alpha = 0.2$ and then $|\Gamma| = 0.0268$. The amplitude distribution in Figure 3(b) is corresponding to this case. These values are used in the following computations.

Figures 5(a)–(c) show the amplitude distributions of the electromagnetic fields near the bend. The waveguide is only just bent without any sorts of devices. In this case, it is seen that the bend causes reflections and produces standing waves of which the VSWR is 3.26.

To suppress the reflections from the bend, the two types of bends are considered. In one type A of the bend, odd number of posts are removed from the corner of the outer sidewall and a straight array of posts are added to close the resulting aperture. Figures 6(a)–(c) show the amplitude distribution of the fields in the type A of bend in case of replacement of three posts. The bend prevents the reflections and the VSWR is 1.12.

The other type B of the bend has an additional post near the corner as shown in Figure 7. Figure 8 shows the VSWR as a function of position x of an addtional post. The right-angle bend with a post located at appropriate position does not cause reflections. The amplitude distributions of the electromagnetic fields near the bend with an additional post at $x = -0.09\lambda$ are shown in Figure 9. It is seen from the figures that almost all incident wave goes around the corner and the bend losses are minimized.

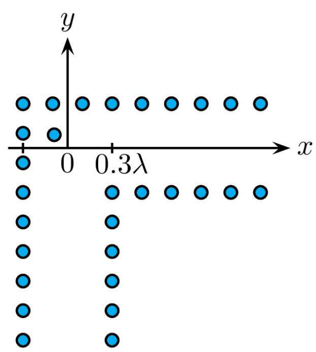

Figure 7: The type B of the bend.

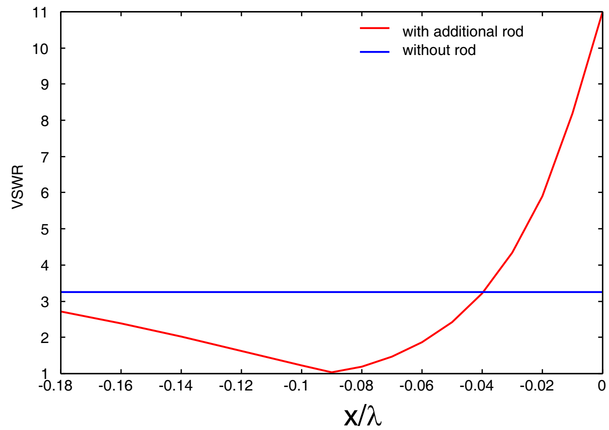

Figure 8: The VSWR for type B of the bend.

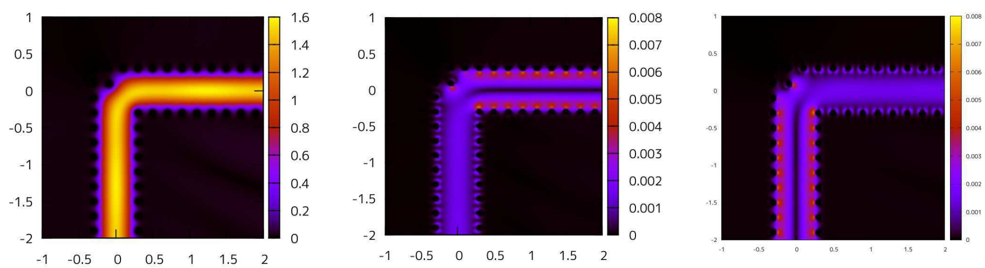

(a) $|Ez|$ (b) $|Hx|$ (c) $|Hy|$

Figure 9: Amplitude distributions of electromagnetic fields near the type B of the bend. The additional post is located at $(-0.09\lambda,\ 0.09\lambda)$.

4. CONCLUSION

The reflection of the guided mode at waveguide bend was examined by the mehod of moments with global basis functions. Only a few additional posts are set at appropriate positions in the post wall waveguide to reduce the bend losses. Especially, only one additional metallic post is enough to minimize the bend losses.

REFERENCES

1. Hirokawa, J. and M. Ando, "Single-layer feed waveguide consisting of posts for plane TEM wave excitation in parallel plates," *IEEE Trans. Antennas Propagat.*, Vol. 46, No. 5, 625–630, 1998.
2. Deslandes, D. and K. Wu, "Single-substrate integration technique of planar circuits and waveguide filters," *IEEE Trans. Microwave Theory Tech.*, Vol. 51, No. 2, 593–596, 2003.
3. Suntives, A. and R. Abhari, "Design and characterization of the EBG waveguide-based interconnects," *IEEE Trans. Adv. Packag.*, Vol. 30, No. 2, 163–170, 2007.
4. Bochra, R., F. Mohammed, and J. Tao, "Design of optimal chamfered bends in rectangular substrate integrated waveguide," *Int. J. Comp. Sci. Iss.*, Vol. 8, No. 2, 376–379, 2011.
5. Yashiro, K., "Global base approach to scattering by conducting circular cylinders," *Proceedings of ICEAA*, 1453–1456, Torino, Italy, September 2013.
6. Abramowitz, M. and I. A. Stegun, *Handbook of Mathematical Functions with Formulas, Graphs, and Mathematical Tables*, 363, Dover, New York, 1972.
7. Lesniewski, P., "Discrete component equivalent circuit for Webster's horns," *Appl. Acoust.*, Vol. 44, No. 2, 117–124, 1995.